

Investigation of a Parametric Instability in a Helicon Discharge by Cross-Correlation Enhanced-Scattering

V. L. Selenin¹, M. Krämer², N. M. Kaganskaya¹ and B. Lorenz²

¹Ioffe Physico-Technical Institute, 26 Polytekhnicheskaya st., St. Petersburg, Russia

²Institut für Experimentalphysik II, Ruhr-Universität Bochum, D-44780 Bochum, Germany

1. Introduction

Enhanced Scattering (ES) of microwaves close to the Upper Hybrid Resonance (UHR) layer is a relatively new back-scattering method using the Extraordinary (X) wave for probing small-scale fluctuations or waves in non-uniform magnetized plasmas [1]. As the scattering takes place close to the UHR where the electric field grows to high values, this method has a high spatial resolution combined with a high sensitivity. Here, we study turbulent density fluctuations in a high-density helicon source where $\omega_{pe} / \omega_{ce} \gg 1$ and thus $\omega_{UHR} \approx \omega_{pe}(x_{UHR})$. As the helicon plasma is immersed in a *homogeneous* magnetic field, the incident probing waves have to tunnel through an evanescent region before entering the UHR.

2. Experiment

The investigations were performed on the large-volume helicon source HE-L ($m = 1$ helical antenna coupling, $\tau_{pulse} = 2 - 3$ ms, $f_{pulse} = 25$ Hz, $P_{RF} < 2$ kW, $f_{RF} = 13.56$ MHz) having the typical plasma parameters $n_e < 2 \times 10^{19}$ m⁻³, $T_e \approx 3$ eV in centre, $T_e \approx 5$ eV at edge, $B_0 < 0.1$ T, $p = 0.1 - 5$ Pa argon gas, $r_p = 7.4$ cm, $L_p = 200$ cm [2]. Electric probe, RF magnetic probes and 1 mm or 8 mm interferometry were applied as additional diagnostics.

To obtain the fluctuation wave number spectra, we apply the Cross-Correlation ES (CES) technique by measuring the phase difference $\Delta\phi = q \Delta x_{UHR}$ (Δx_{UHR} : distance between the UHR layers, q : wave number) between two back-scattered signals differing in probing frequency and, thus, coming from different scattering layers [3,4]. We used frequencies around 9 GHz and 28 GHz corresponding to the measuring (UHR) positions at the plasma boundary and the centre of our helicon source HE-L, respectively. The typical parameters for the CES measurements at the plasma edge were $B_0 = 50$ mT, $n_e(r=0) = 1 \times 10^{19}$ m⁻³; the centre probing frequency $F_1 = 9.4$ GHz corresponds to $n_e \cong 10^{18}$ m⁻³ UHR density and the UHR layer 2 cm apart from the wall, where the gradient scale length $L_n \cong 1.8$ cm, $\kappa = k_0 \cdot \text{width of cut off region} \approx 0.8$. For $F_1 = 28$ GHz the UHR is localized close to the plasma centre where the local density equals 10^{19} m⁻³.

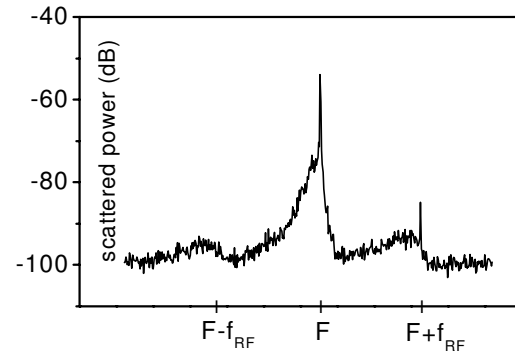
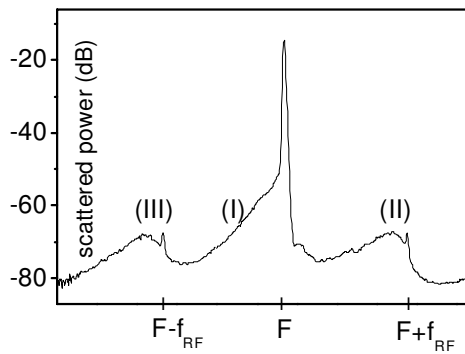


Fig.1a. Frequency spectra for $f_{RF} \approx 9$ GHz Fig.1b. Frequency spectra for $f_{RF} \approx 28$ GHz

The frequency spectra integrated over all fluctuation wave numbers q are shown for both probing bands in Fig.1. The narrow line in the center is associated with the reflected probing power and, hence, corresponds to the probing frequency. The spectra are similar and consist of a continuous *red*-shifted sideband decreasing with frequency (part I) and two rather broad maxima close to the pump frequency f_{RF} (parts II and III) at both sides of the probing peak.

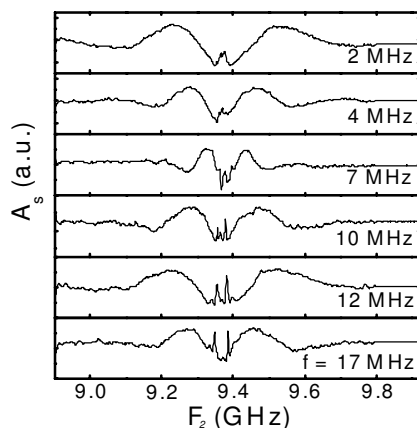


Fig.2a: Output signals of CES circuit ($F_1 = 9.4$ GHz)

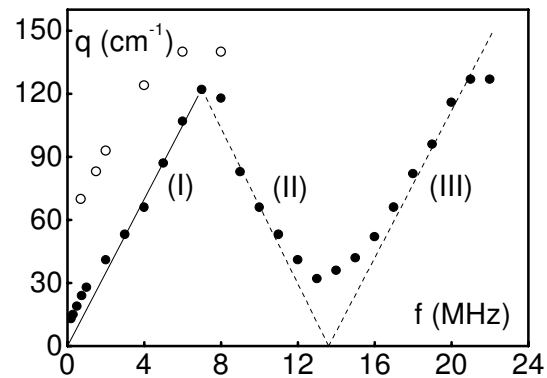


Fig.2b: Dispersion relation (full circles: 9.4 GHz, open circles: 28 GHz)

To measure the fluctuation wave numbers, we used two frequency channels with homodyne conversion. One oscillator has a fixed frequency, while the frequency of the other was varied thus providing a radial scan of the UHR. In Fig.2a, we show that the signals are proportional to the cosine of the mean phase difference between the signals in the channels for different spectral components of the fluctuations in the probing frequency range ($f_{RF} \approx 9$ GHz); similar results were obtained for the 28 GHz band. The fluctuation wave numbers, obtained from the period of these curves are plotted in Fig.2b: Different parts of the dispersion curve, (I), (II), (III), correspond to different parts of the frequency spectrum (see Fig.1). The solid lines follow to the ion-acoustic dispersion relation corresponding to the temperatures $T_e = 4.7$ eV at the boundary and $T_e = 3$ eV in the centre of the plasma. Yet, the agreement between the pre-

dicted and measured dispersion relations is only good for the boundary. The discrepancy for the plasma centre may be due to the fact that the fluctuations have much higher amplitudes (nonlinear effects) and a smaller coherence length. Hence, part (I) of the dispersion curve can be attributed to ion-sound turbulence in both cases. The *red*-shifted part (I) in the frequency spectra (Fig.1) is associated with turbulent fluctuations propagating mainly toward the plasma edge while part (II) corresponds to fluctuations propagating in opposite direction, i.e., inwards. The different parts of the spectra are intimately related with each other which can particularly be seen from the dispersion curves in Fig. 2b. It turns out that the parts (I) and (II) fulfill the frequency and wave number selection rules that is typical for a parametric decay. Possible is a decay of helicon modes into ion-sound and Trivelpiece-Gould waves having large perpendicular wave numbers (as compared to the helicon modes), but different signs. In this case, part (III) can be attributed to coalescence of helicon and ion-sound waves.

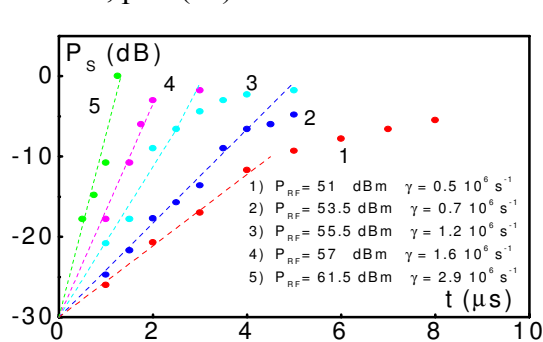


Fig.3a. Growth of density fluctuations

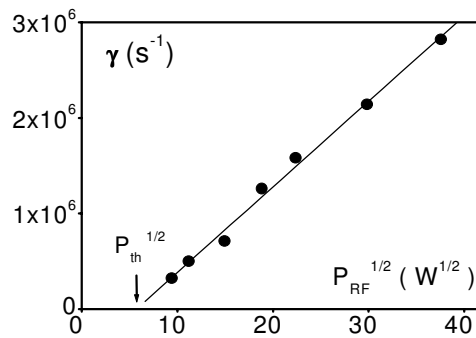


Fig.3b. Power dependence of growth rate

Evidence for a parametric instability shows also Fig.3 where we plotted the growth of the scattered signal for different RF powers. We can deduce the growth rate that is proportional to the square root of the RF power and, thus, to the field strength of the helicon pump, i.e., $\gamma \propto (P / P_{th})^{1/2} - 1$. Growth rates up to $\gamma \approx 5 \times 10^6 \text{ s}^{-1}$ were measured in our experiments.

The nonlinear nature of the fluctuations and their role for the electron heating is evidenced by measurements carried out with variable RF power. We applied a second RF pulse 20 μs after the main pulse varying the RF amplitude. From Fig. 4 we see that the scattered signal reveals a threshold dependence on the RF power: When the turbulence saturates, the density grows steeply, obviously due to stronger electron heating and thus a higher ionisation rate. We therefore conclude that the saturation mechanism may be associated with energy transfer from helicon modes to the plasma electrons via turbulence.

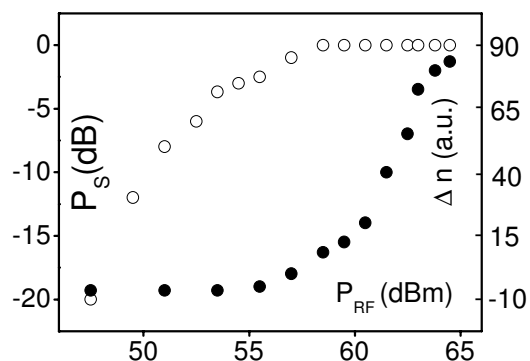


Fig.4. Scattered power (open circles) and density increase (full circles) vs. RF power

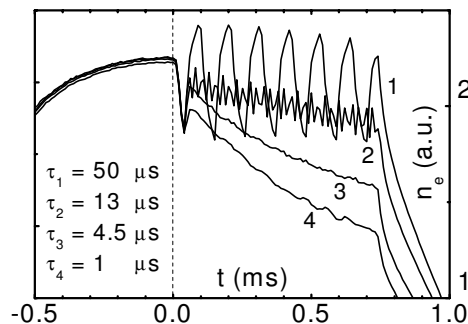


Fig.5. Variation of plasma density increase produced by burst of RF pulses with different durations τ ; $r_{\text{measurement}} \approx 25$ mm.

This finding is supported by another experiment. We applied a burst of RF pulses with different duration τ , but constant duty cycle (50%) thus keeping the mean RF power constant. We have plotted the plasma density measured by a Langmuir probe close to the plasma centre in Fig.5. If the pulse duration is long enough as compared to the ionisation time, $1/\nu_I$ (curve 1, $\tau = 50 \mu\text{s}$), the density grows to a maximum during each pulse and decreases when the RF power is off. (Note that, because of the better matching during the RF burst phase, the maximum density exceeds the density in the first pulse.). From the slope of the density at the beginning of the RF pulse we deduce an ionisation time of about $80 \mu\text{s}$ corresponding roughly to the electron heating time. From this value we calculate $T_e \approx 4$ eV in the first period of the RF pulse. For $\tau = 13 \mu\text{s}$, there is only a slight modulation of the density evolution (curve 2) and for $\tau = 4.5 \mu\text{s}$ and $\tau = 1 \mu\text{s}$, the density decreases smoothly. Comparing the four density curves (curves 1 and 2 averaged over the pulse period) it turns out that the plasma decay time increases with the pulse duration. Obviously, the ionisation frequency ν_I increases as well, and as ν_I is strongly correlated with the electron heating and, hence, with the RF power absorption, we conclude that the electrons absorb the RF energy more effectively when the RF pulses are longer. This can be accounted for the turbulent electron heating gradually increasing with evolution of the turbulence.

Acknowledgements

This work was supported by the *Deutsche Forschungsgemeinschaft* through the Project KR 1058 and the *Russian-German Cooperation*, Contract 146 RUS 590.

References

- [1] K.M. Novik and A.D. Piliya, *Plasma Phys. Control. Fusion* 35, 357 (1994).
- [2] M. Krämer, Th. Enk and B. Lorenz, *Physica Scripta* T84, 132 (2000).
- [3] E.Z. Gusakov, N.M. Kaganskaya, M. Krämer, V.L. Selenin, *Plasma Phys. Contr. Fusion* 42, 1033 (2000).
- [4] N. M. Kaganskaya, M. Krämer, V. L. Selenin, *Physics of Plasmas* 8, 4694 (2001).